Available online at www.sciencedirect.com

SCIENCE DIRECT®

Journal of Molecular Catalysis A: Chemical 203 (2003) 241–250

JOURNAL OF MOLECULAR CATALYSIS A: CHEMICAL

www.elsevier.com/locate/molcata

Effects of the method of preparing titanium pyrophosphate catalyst on the structure and catalytic activity in oxidative dehydrogenation of *n*-butane

Ioan-Cezar Marcu [a,1], Ioan Sandulescu [a,1], Jean-Marc M. Millet [b,*]

[a] *Département de Technologie Chimique et Catalyse, Faculté de Chimie, Université de Bucarest 4-12, Blv. Regina Elisabeta, 70346, Bucarest, Romania*

[b] *Institut de Recherches sur la Catalyse, CNRS, associé à l'Université Claude-Bernard Lyon I, 2 Avenue Albert Einstein, F-69626 Villeurbanne Cedex, France*

Received 12 March 2003; accepted 9 April 2003

Abstract

Five different preparation methods have been developed to synthesize titanium pyrophosphate (TiP_2O_7) which are active and selective catalysts for oxidative dehydrogenation of *n*-butane into butene and butadiene. The crystallinity, surface area, reducibility by *n*-butane and acid–base properties appeared different depending upon the method used. The activity of the catalysts in the oxidative dehydrogenation of *n*-butane appeared to depend mostly upon their redox properties whereas the selectivity was influenced by their acidic properties. Both properties seemed to be correlated to the crystallinity of the compounds but not to their surface area.
© 2003 Elsevier Science B.V. All rights reserved.

Keywords: Titanium phosphate; Oxidative dehydrogenation; *n*-Butane; Butene; Butadiene

1. Introduction

Fewer studies have been conducted on the oxidative dehydrogenation of *n*-butane compare to other light alkanes. This is mainly due to the lack of interest of petrochemical companies to develop a new process for the production of butadiene. This situation is caused by the surplus of butadiene produced as a by-product of ethylene and for which the demand is not increasing as fast as the demand for ethylene [1]. However, butadiene could find in the future new applications that would boost its production and regain interest for new routes of synthesis like the direct oxidative dehydrogenation of *n*-butane.

As recently pointed there is a lack of information about the role and extend of the homogeneous reaction of *n*-butane with oxygen [2]. The results of several studies, claiming high yields of butene and butadiene at temperature higher than 813 K, should be considered carefully because of substantial noncatalytic dehydrogenation [3].

It has been shown in previous studies that titanium pyrophosphate was a very active and selective catalyst for the oxidative dehydrogenation of *n*-butane to butene and butadiene [4,5]. With a maximum conversion of 25% and selectivity in dehydrogenation products of 56%, it is an almost as efficient catalyst as the

* Corresponding author. Tel.: +33-72445317; fax: +33-72445399.
E-mail address: millet@catalyse.univ-lyon1.fr (J.-M.M. Millet).
[1] Tel.: +40-21-4103178x138; fax: +40-21-3159249.

1381-1169/03/$ – see front matter © 2003 Elsevier Science B.V. All rights reserved.
doi:10.1016/S1381-1169(03)00376-5

VMgO catalyst for that reaction, although it produced less butadiene compared to butenes [3,6].

In order to get fundamental information about this catalyst, we have perfected five different methods to prepare it. In this paper, these methods are described and the solids obtained characterized in terms of crystallinity, surface area, reducibility by *n*-butane and acidity. These parameters are discussed in relation with results for *n*-butane oxidative dehydrogenation.

2. Experimental

2.1. Preparation of the catalysts

Five kinds of titanium pyrophosphate catalysts were prepared according to the following procedures:

- *Method 1 (M1)*: Titanium dioxide (reference Rhône-Poulenc) was reacted with phosphoric acid (85%). The two compounds were mixed until homogeneous slurry was formed; it was then dried at 393 K and calcined at 973 K for 2.5 h.
- *Method 2 (M2)*: Method M2 was inspired from a method described by Ai [7], It was based upon the reaction between a solution containing 580 ml of water, 40 ml of lactic acid (85%), 5 ml of NH_3 (28%) and 25.60 g of $TiCl_4$ and a solution of phosphoric acid (106 g, 30%) added drop-wise. The gel obtained was separated by centrifugation and dried between 353 and 473 K with a gradual increase of temperature over 6 h. The obtained solid was calcined under air at 573, 723 and 873 K for 6 h at each temperature.
- *Method 3 (M3)*: The starting procedure was the same as for M2 but the gel obtained was separated from the excess of water by a slow evaporation under flowing air and stirring at room temperature. After evaporation of the excess of water, the remaining gel was dried and calcined as described in the M2 method protocol.
- *Method 4 (M4)*: A titanium di-isopropoxide bis(2,4-pentanedionate) solution in isopropyl alcohol (IPA) was hydrolyzed with an aqueous solution of H_3PO_4 0.3 M at a pH maintained at 9 by addition of an ammonia solution. The resulting gel was recovered by centrifugation and repeatedly washed with distilled water, then dried in air at 333 K and eventually calcined at 923 K.
- *Method 5 (M5)*: Method M5 was described in literature [8]. A titanium tetra (*sec*-butoxide) solution in *sec*-butanol was hydrolyzed with H_3PO_4 1 M in *sec*-butyl alcohol. The resulting gel was dissolved in concentrated H_3PO_4 (85%) to obtain a molar ratio P/Ti equal to 10. After some hours of stirring at room temperature, a white gel appeared which was stirred for 3 days. The solid was recovered by centrifugation and repeatedly washed with distilled water, air dried at 333 K and finally calcined at 923 K for 4 h.

2.2. Physico-chemical characterization of the catalysts

Powder X-ray diffraction (XRD) patterns were obtained using a BRÜKER D5005 diffractometer and Cu Kα radiation. They were recorded with 0.02° (2θ) steps over the 3–80° angular range with 1 s counting time per step. Metal contents of the solids were determined by atomic absorption (ICP) and specific surface areas measured by the BET method using nitrogen adsorption. IR spectra were recorded with an Fourier-transform infrared (FTIR) spectrometer (IFS110 BRÜKER) using the KBr pellet technique for sample preparation. XPS measurements were performed with a VG ESCALAB 200 R. Charging of samples was corrected by setting the binding energy of adventitious carbon (C 1s) at 284.5 eV. The conditions of electron spin resonance (ESR) have been described elsewhere [4]. The spectra have been recorded at 77 K using a Varian E9 spectrometer operating in the X-band mode. Diphenylpicrylhydrazil (DPPH) was used as a standard for *g*-values determinations using a dual cavity and vanadyl sulfate for spin calibration.

The surface acidity of the catalysts was investigated by means of both IPA dehydration reaction test and FTIR spectroscopic study of pyridine adsorption. The IPA dehydration reaction was conducted at 473 K in a quartz flow micro-reactor fed with N_2 saturated with IPA ($30\,cm^3\,min^{-1}$). Two hundred seventy milligram of catalyst were accurately weighted and loaded into the reactor and heated overnight at the desired temperature in N_2 flow prior to starting the catalytic runs. The products were analyzed by gas chromatography using a Poraplot Q column. Because all the catalysts were undergoing a deactivation during the first 3 h, the catalytic data were only collected after at least

4 h (242 min). Pyridine FTIR spectra were recorded in a IFS110 BRÜKER spectrometer. The samples were pressed into self-supporting discs, placed in an IR cell, and treated at 803 K successively under oxygen for 8 h and under vacuum (1.33×10^{-3} Pa) for 1 h. After cooling to room temperature, the samples were exposed to pyridine vapor for 5 min. Then, the spectra (200 scans, 1 cm^{-1} resolution) were recorded after evacuation (1.33×10^{-3} Pa) for 30 min at room temperature, 373, 423, 473, 523 and 573 K.

2.3. Catalytic testing

The oxidative dehydrogenation of *n*-butane was performed in a fixed-bed reactor operating at atmospheric pressure. The apparatus and the conditions have been described elsewhere [4]. The catalytic tests were conducted for at least 12 h and the catalysts were recovered after catalytic test by cooling them down rapidly in the flow of reactants from 803 K.

A gas feed with an air to *n*-butane ratio equal to 5 and a VVH of 1000 h^{-1} with respect to *n*-butane were used. The major products formed under these reaction conditions were 1- and 2-butenes, butadiene, CO, CO_2, and cracking products (methane, ethane, ethylene and propylene).

3. Results

3.1. Chemical analyses, BET surface area measurements and X-ray diffraction analyses

The physico-chemical characteristics of the prepared titanium pyrophosphates are presented in Table 1. The P/M ratios obtained from chemical analysis were all close to the theoretical ones. The specific surface areas were low except that of the solid prepared using method M2. The later appeared to be uncommonly high for pyrophosphates. Although this surface area was very high, the pore volume of this solid was small (0.33 $cm^3\,g^{-1}$), with pore size corresponding to that of mesopores. The adsorption isotherm of this solid showed a hysteresis loop (Fig. 1) classified as type IV by IUPAC [9]. The X-ray diffraction patterns of the prepared compounds are displayed in Fig. 2. The solids prepared using methods M1, M3 and M5 were crystallized phases whereas those prepared using methods M2 and M4 were amorphous.

Table 1
The physico-chemical characteristics of the catalysts

Catalyst	Surface area ($m^2\,g^{-1}$)		P/Ti ratio	
	Before test	After test	Bulk (ICP)	Surface (XPS)
TiP_2O_7-M1	6.0	6.7	1.9	3.4
TiP_2O_7-M2	107.4	77.1	1.9	2.8
TiP_2O_7-M3	18.3	18.5	2.0	4.2
TiP_2O_7-M4	3.1	3.4	2.1	4.0
TiP_2O_7-M5	8.3	8.2	2.0	3.7

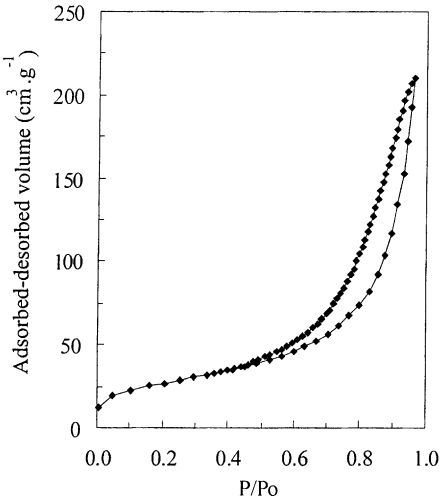

Fig. 1. Adsorption isotherm of TiP_2O_7-M2.

3.2. Surface chemical analyses

The surface composition of the catalysts was investigated by XPS (Table 1). All the catalysts presented a P/Ti surface ratios higher than the bulk ratio. Such feature is common to almost all phosphates and has been reported for iron and vanadium pyrophosphates based catalysts [10,11]. The P/O ratios were superior to 1:4, which could be due to the presence of pyro or polyphosphate anions on the surface.

3.3. Infrared and electron spin resonance spectroscopy

The infrared spectra of the samples in the 500–2000 cm^{-1} range are presented in Fig. 3. The spectra of the crystallized solids (M1 and M5) exhibited

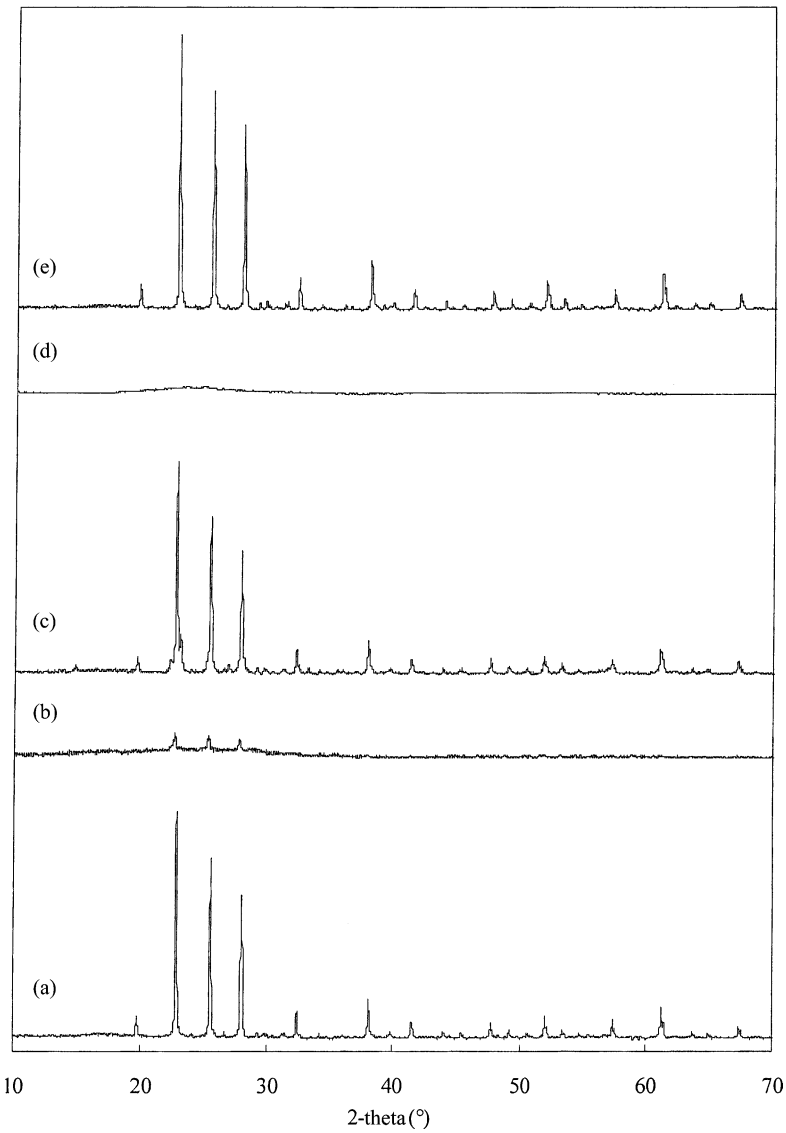

Fig. 2. X-ray diffraction patterns of the pyrophosphate catalysts before catalytic test: (a) TiP_2O_7-M1; (b) TiP_2O_7-M2; (c) TiP_2O_7-M3; (d) TiP_2O_7-M4; and (e) TiP_2O_7-M5.

a broad maximum between 1000 and 1200 cm^{-1}, assigned to P–O vibrations, two bands towards 960 and 745 cm^{-1}, attributed to P–O–P vibrations and two bands at 623 and 563 cm^{-1}, assigned to O–P–O vibrations [12]. In the case of amorphous solids (M2 and M4), the same bands but broader were observed. The band between 1000 and 1200 cm^{-1} was particularly large and consequently, the band at 960 cm^{-1} appeared only as a shoulder. Moreover, the maximum of this broad band shifted to lower frequencies indicating an increase of the P–O distances. We also observed a broad maximum towards 745 cm^{-1} and two others centered at 610 and 563 cm^{-1}.

TiP_2O_7-M1, -M2, -M3 and -M4 catalysts have been studied by ESR at 77 K. The synthesized solids were pretreated under oxygen at 823 K. The cell was

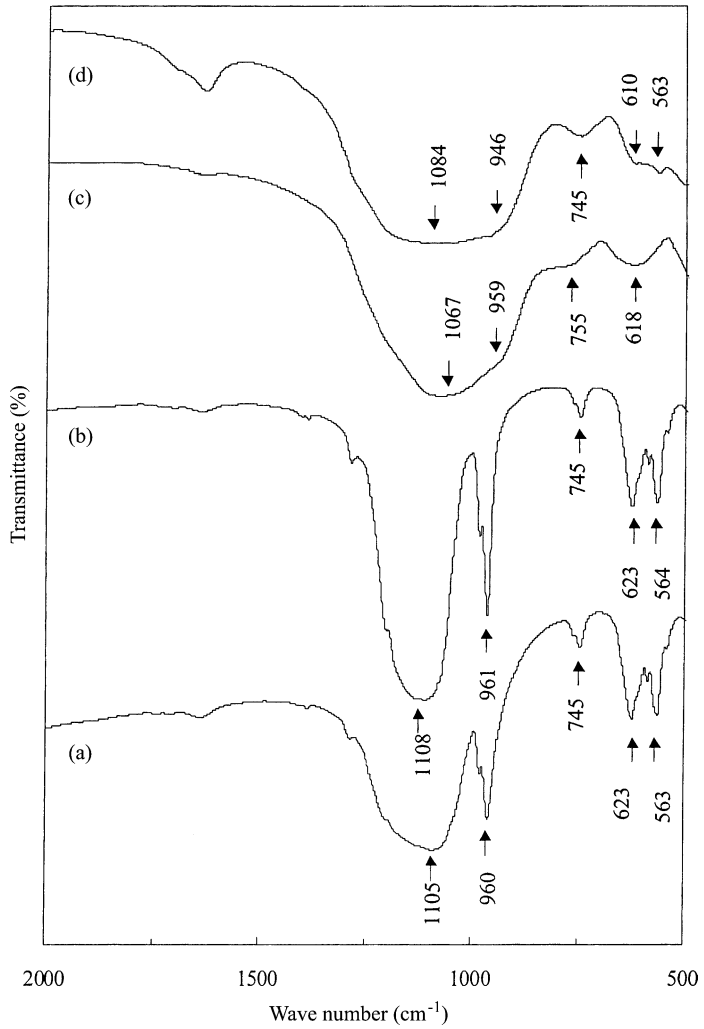

Fig. 3. Fourier-transform IR spectra (KBr pressed disks) of TiP_2O_7-M1 (a), TiP_2O_7-M5 (b), TiP_2O_7-M4 (c) and TiP_2O_7-M2 (d).

then evacuated and cooled down to 77 K and the ESR spectrum recorded. The spectra obtained for TiP_2O_7-M2, -M3 and -M4 were rather similar to that of TiP_2O_7-M1 given in Fig. 4 (spectrum a). Two signals with a very low intensity corresponding to trivalent titanium ions were observed. The first signal (1) was characterized by a giromagnetic factor $g = 1.97$ and the second (2) by $g_{\|} = 1.93$ and $g_{\perp} = 1.82$. From the literature, these signals have, respectively, been attributed to Ti^{3+} cations into interstitial positions and to Ti^{3+} cations neighboring an oxygen vacancy [13]. The treatment under *n*-butane (2.66 kPa at 823 K for 30 min) led to the appearance of a third signal (3) with *g*-value close to that of free electron. It was attributed to carbon species deposited on the surface [13]. With the treatment, a strong increase in intensity of signal (2) was also observed whereas signal (1) remained unchanged (spectrum b). This demonstrates that *n*-butane could reduce titanium in the pyrophosphates at the catalytic reaction temperature. After a subsequent treatment under oxygen at 823 K, signal (3) strongly decreased and signal (2) regained its starting intensity (spectrum c) which clearly showed that such reduction was reversible. Finally, the four catalysts have been compared in terms of reduction extent after treatment at 823 K [4]. Different reduction extents, normalized

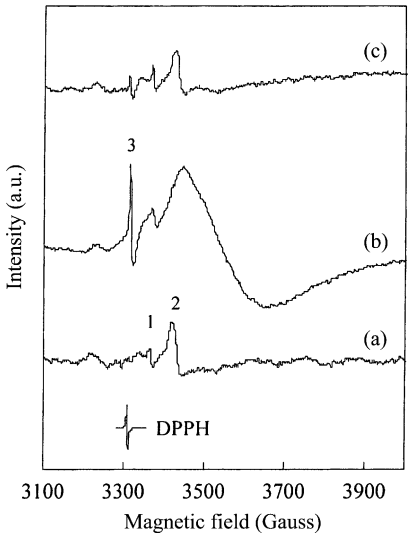

Fig. 4. ESR spectra recorded at 77 K of the TiP_2O_7-M1 compound (a) before treatment under *n*-butane, (b) after treatment under *n*-butane at 823 K and (c) after reduction and re-oxidation under oxygen at 823 K.

with respect to the surface area have been observed depending upon the type of titanium pyrophosphates (Table 2).

3.4. Pyridine desorption and isopropyl alcohol dehydration experiments

Pyridine (Py) desorption followed by infrared spectroscopy and IPA dehydration reaction test have been used to characterize the acidity of the pyrophosphate catalysts. The infrared spectra of pyridine adsorbed on the samples M1, M2 and M4 were recorded after treatment at different temperatures between 298 and 573 K. The IR spectra of Py adsorbed on the three catalysts TiP_2O_7-M1, -M2 and -M4 were taken following outgassing at room temperature, 373, 423, 473, 523 and 573 K. They are presented, respectively, in Fig. 5a–c. The bands at 1609, 1577, 1491 and 1448 cm^{-1} are typical of pyridine chimisorbed on Lewis acid sites. The bands at 1640 and 1544 cm^{-1} are typical of pyridinium cations whose presence confirms that of Brønsted sites [14,15]. All the bands reported above are observed in the spectra with variation in position that did not exceed 2 cm^{-1}, which showed that the three solids were rather similar. A measure of the υ(8a) vibration (1578 cm^{-1} in the liquid) may be taken as a measure of the strength of the Lewis sites [16]. In our case, the frequency of 1609 cm^{-1} was a clear indication of the presence of medium strong sites. Concerning the Brønsted sites, it is important to note that the protonation of a relatively weak base such as pyridine is an indication of their relevant strength. Moreover, the stability of the pyridinium cations even after evacuation at 573 K is a further indication that the sites were rather strong. Upon outgassing at increasing temperatures, the intensities of all the bands decreased; this was more pronounced after 473 K.

Figs. 6 and 7 show, respectively, the evolution of the Brønsted and Lewis relative acidity as a function of temperature, expressed as area under the peak at 1544 and 1447 cm^{-1} and normalized by surface unit. The Brønsted acidity of the samples decreased in the order M1 (0.68) > M2 (0.41) > M4 (0.32), and Lewis acidity, in the order M4 (1.72) > M2 (0.37) > M1 (0.29). The numbers into brackets correspond to the normalized surface areas under the peaks expressed in arbitrary units, in the spectra recorded after evacuation at 423 K.

The catalytic decomposition of IPA was studied on two crystallized (M1 and M5) and two amorphous samples (M2 and M4). The results obtained at 473 K are reported in Table 3. Over all of the compounds, only the formations of propene, and di-isopropylether (DIPE) were observed. No acetone was detected in the product mixtures. Because all the catalysts were undergoing a small deactivation during the first hours, the catalytic data were collected after 242 min. Propene was the major product of the reaction of the IPA dehydration, which demonstrates the acid character of the catalysts. Based on the intrinsic rate of propene formation, the acidity of the titanium pyrophosphates decreased in order M2 > M1 > M5 > M4. It is

Table 2
ESR parameters of the Ti^{3+} species and spin numbers per unit of surface area, calculated for the different compounds reduced at 773 K under *n*-butane

Compound	Components of the magnetic tensor *g*		Number of spin (m^{-2})
	$g_{\parallel}$	$g_{\perp}$	
TiP_2O_7-M1	1.93	1.82	6.2×10^{17}
TiP_2O_7-M2	1.93	1.84	2.1×10^{17}
TiP_2O_7-M3	1.92	1.79	4.2×10^{17}
TiP_2O_7-M4	1.92	1.80	4.7×10^{17}

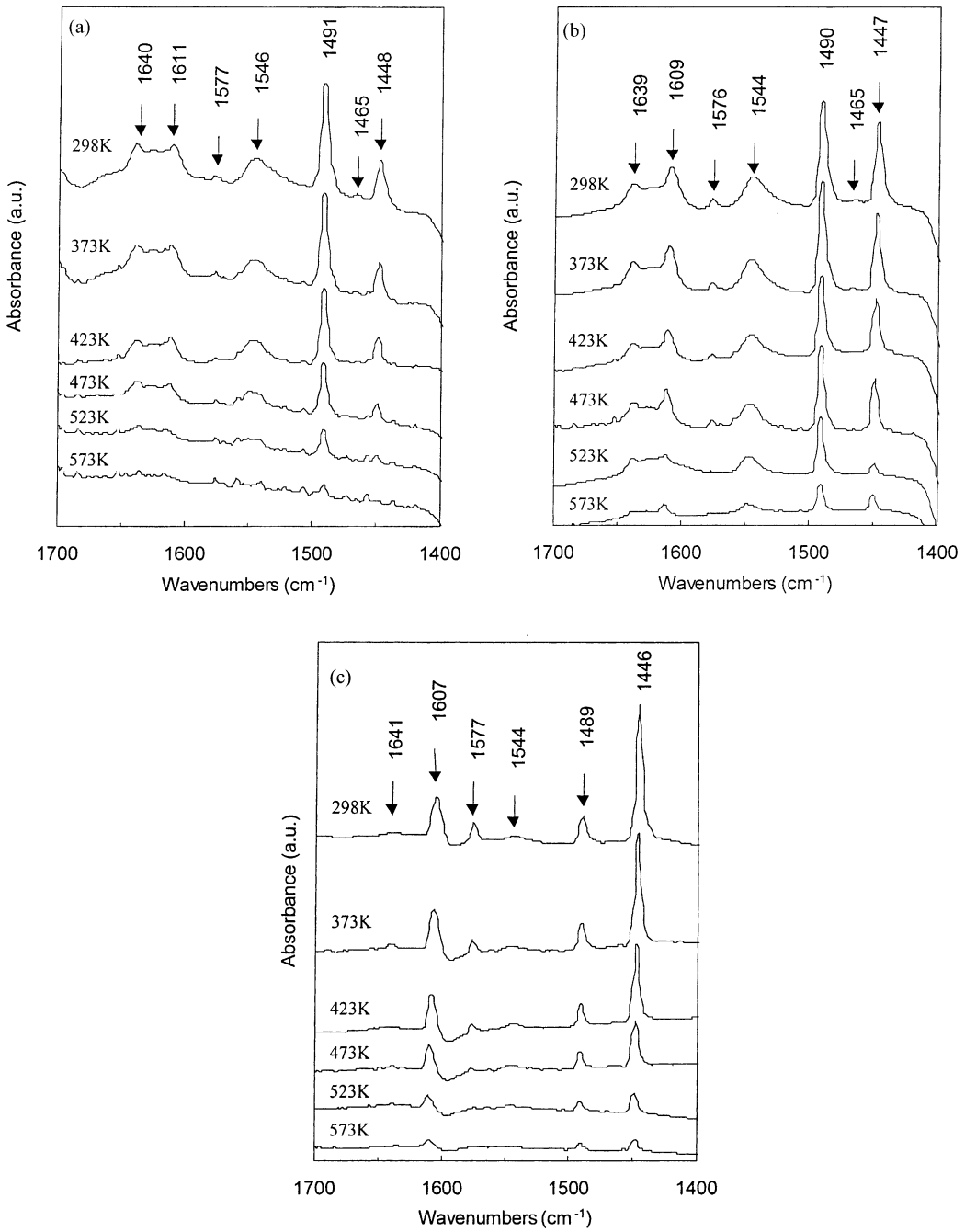

Fig. 5. FTIR spectra (normalized by surface unit) of the surface species after pyridine adsorption and outgassing at indicated temperatures on: (a) TiP_2O_7-M1; (b) TiP_2O_7-M2; and (c) TiP_2O_7-M4.

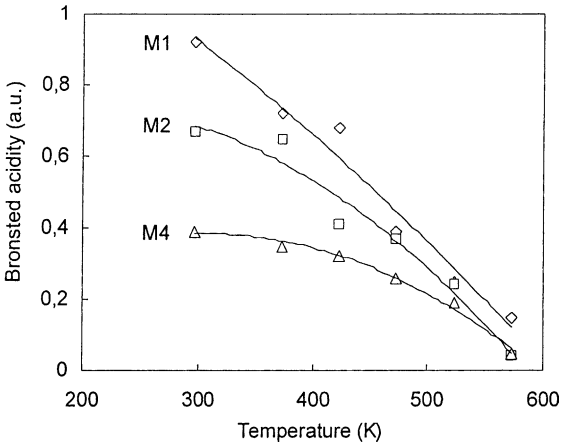

Fig. 6. Relative variation of the area of the Brønsted (1540 cm^{-1}) pyridine band as a function of the temperature of desorption for the pyrophosphates M1, M2 and M4.

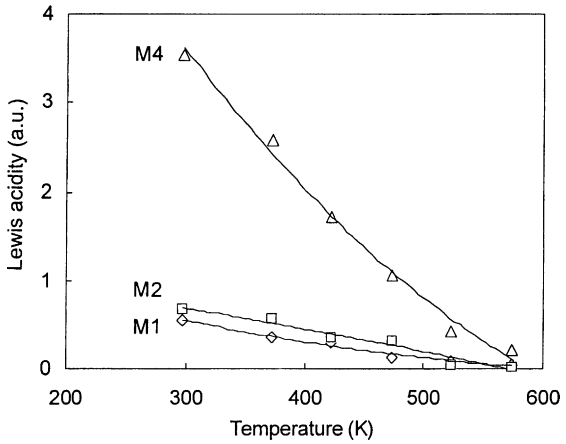

Fig. 7. Relative variation of the area of the Lewis (1450 cm^{-1}) pyridine band as a function of the temperature of desorption for the pyrophosphates M1, M2 and M4.

interesting to note that DIPE was formed on the crystallized solids but almost not on the amorphous ones.

3.5. Catalytic oxidative dehydrogenation of n-butane

The catalytic properties of the titanium pyrophosphates were determined in the range 683–883 K. The results obtained at 763 and 803 K are gathered in Table 4. The prepared solids presented very different activities but were all selective towards oxidative dehydrogenation products with systematically maximum yields around 803 K.

The three crystallized solids (M1, M3 and M5) had comparable catalytic properties although M1 appeared more active than the two others. Concerning the two amorphous solids (M2 and M4), the conversion on M2 was comparable to that on the crystallized solids, but not that on M4 which was very low. However, the activity of the latter, expressed as the intrinsic rate of *n*-butane transformation, was comparable to those of the other pyrophosphates. This could be interpreted by the fact that M4 presented sites as active as those of the crystallized pyrophosphates, but with a smaller density per surface area unit. Furthermore, it can be seen that these sites were less selective towards butadiene. On the other side, M2 presented the lowest activity. Its surface area was however very high and to explain the level of conversion observed on this catalyst, the density of active sites per surface area unit should also be rather low. The conversion level was approximately the same on the different pyrophosphates except for M4 and the selectivities observed on the formers can directly be compared to each other. We can see that the compounds have very similar selectivities. On M2, the selectivity of CO_x was slightly

Table 3
Results of the dehydration of isopropanol on titanium pyrophosphates

Catalyst	Isopropanol conversion (%)	Selectivity (%)		v_i (10^{-10} mol s^{-1} m^{-2})[a]	
		Propene	DIPE	Propene	DIPE
TiP_2O_7-M1	6	87	13	215	32
TiP_2O_7-M2[b]	31	99	1	851	9
TiP_2O_7-M4	1	96	4	79	3
TiP_2O_7-M5	7	82	18	177	39

[a] Intrinsic rate of propene and di-isopropylether (DIPE) formation.
[b] Mass tested: 32 mg.

Table 4
Catalytic performances of TiP_2O_7 catalysts in oxidative dehydrogenation of *n*-butane

Catalyst	Temperature (K)	*n*-Butane conversion (%)	Selectivity (%)					1-C_4'/2-C_4'[a]	Rate of *n*-butane transformation ($\times 10^{-8}$ mol s^{-1} m^{-2})
			Butenes	Butadiene	TDS[b]	Cracking products	CO_x		
TiP_2O_7-M1	763	20	43	12	55	18	28	0.5	48
	803	25	42	14	56	22	22	0.5	60
TiP_2O_7-M2	763	14	41	10	51	7	42	0.5	4
	803	18	39	15	54	12	34	0.6	5
TiP_2O_7-M3	763	25	39	15	54	17	29	0.5	35
	803	28	33	14	47	32	21	0.6	39
TiP_2O_7-M4	763	3	41	2	43	18	39	0.4	29
	803	5	34	4	38	27	35	0.4	47
TiP_2O_7-M5	763	17	39	11	50	21	29	0.5	34
	803	22	37	14	51	22	27	0.5	44

[a] 1-C_4': 1-butene; 2-C_4': *cis*- and *trans*-2-butenes.
[b] Total Dehydrogenation Selectivity.

higher and that of cracking products lower. The ethylene to ethane ratio characterizing the cracking products distribution was lower for this catalyst compared to others (17 instead of 26 ± 2) and it may be proposed that ethylene was oxidized in the pores, which presence was related to the high surface area of this compound (Table 1, Fig. 1). Since the selectivity to oxidative dehydrogenation products from alkanes always decreases when conversion level increases, M4 may be considered as a lot less selective for these products than the other catalysts.

4. Discussion

The different methods used to prepare the titanium pyrophosphates led to different compounds. All these compounds have the right composition and correspond to pyrophosphates as clearly shown by IR spectroscopy but they are either crystallized or amorphous and exhibit surface areas ranging from 3 to 107 m^2 g^{-1}. These later characteristics did not seem to depend from one another even if none of the methods led to crystallized solids with high surface area. No relation appears neither to exist with the surface composition of the solids nor their acidic properties.

No correlation between the acidity of the solids measured from the IPA dehydration reaction test and from the pyridine desorption was observed. This is probably due to the deactivation of the catalyst at the begining of the dehydration reaction test. It is also possible that, in the case of TiP_2O_7-M2, the isopropanol conversion level was too high for comparing the acidity of this catalyst to the others. It is interesting to note that DIPE was preferentially formed on the amorphous catalyst rather than on the crystallized ones. The formation of this product should thus not only be related to the acidity of the compound but also to a given structural arrangement leading to the neighboring of two sites allowing adsorption of two close alcohol molecules and their reaction.

The catalytic properties of the different pyrophosphates can be related to both redox and acid–base properties. It is worth noting that when the reduction extent by *n*-butane measured by ESR on different catalysts was plotted as a function of the intrinsic rate of *n*-butane conversion, a linear relationship was observed (Fig. 8). This lead to the conclusion that the activity of the catalysts depends almost exclusively of the ability of the titanium to undergo oxido-reduction. It is also in agreement with the results previously published showing that the limiting step in *n*-butane conversion on these compounds was the re-oxidation of the catalysts [5]. Neither the crystallinity nor the surface area of the compounds seem to influence these redox properties and no relation can neither be found with the acidic properties. It can be noted that the results of the catalytic test of the solids lead to the conclusion that the site density, i.e. number of sites per surface area unit, on the amorphous compounds is lower that

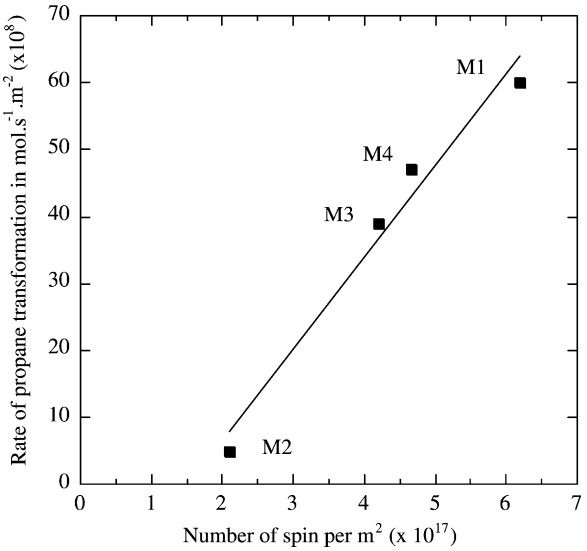

Fig. 8. Dependence of the intrinsic rate of *n*-butane conversion at 803 K on the reduction extent of the titanium pyrophosphates determined at 823 K.

on the crystallized ones but that these sites have on both type of compounds the same intrinsic activity.

The selectivity of the catalysts appears strongly influenced by their Lewis acidity. The more acid catalyst M4 is the least selective for the oxidative dehydrogenation of *n*-butane. Strong Lewis acid sites may absorb strongly the reactions intermediates or butenes and butadiene that are rather basic molecules and lead to their total oxidation. No clear relation has been observed between the P/Ti surface ratio and the acidity of the compounds. It seems that Lewis acidity increases with P/Ti whereas Brønsted acidity decreases. Similarly, no relation exists with the crystallinity or the surface area.

A correlation between the selectivity in DIPE and the crystallinity is observed when the dehydration of isopropanol is studied on the samples. The selectivity to DIPE is high when the solids are amorphous. Surface structure defects on such compounds may lead to the neighboring of two alcohol adsorption sites that would be responsible for this special catalytic property.

5. Conclusion

The findings obtained in this study are summarized as follows:

- The crystallinity, surface area and atomic P/Ti surface ratio of the studied titanium pyrophosphate catalysts were different depending upon the method used to prepare them, and this was independent of the nature of the starting titanium precursor.
- All the studied pyrophosphates underwent a reduction under *n*-butane at 773 K and a linear relationship was observed between their reduction extent by *n*-butane and their intrinsic rate of *n*-butane conversion; however this was not correlated with the surface area nor with the crystallinity of the catalysts. This result confirmed that the re-oxidation of the catalysts was the rate determining step of the reaction
- The Lewis acidity of the catalysts appeared to significantly influence the catalytic properties, the greater acidity was correlated with the less selective catalysts. Inversely, the Brønsted acidity did not appear correlated with any catalytic properties in the oxidative dehydrogenation of *n*-butane.

References

[1] B. Torck, L'Act. Chim. (I) 4 (1997) 3.
[2] L.M. Madeira, M.F. Portela, Catal. Rev. 44 (2) (2002) 247.
[3] H.H. Kung, Oxidative dehydrogenation of light alkanes, in: D.D. Eley, H. Pines, W.O. Haag (Eds.), Advances in Catalysis, vol. 40, Academic Press, New York, 1994, p. 1.
[4] I.C. Marcu, I. Sandulescu, J.M.M. Millet, Appl. Catal. 227 (2002) 309.
[5] I.C. Marcu, J.M.M. Millet, J.M. Herrmann, Catal. Lett. 78 (2002) 273.
[6] J.M. Lopez Nieto, A. Dejoz, M.I. Vasquez, W.O. Leary, J. Cinningham, Catal. Today 40 (1998) 215.
[7] M. Ai, Appl. Catal. 48 (1989) 51.
[8] J. Santamaria-Gonzalez, M. Martinez-Lara, M.A. Banares, M.V. Martinez-Huerta, E. Rodriguez-Castellon, J.L.G. Fierro, A. Jimenez-Lopez, J. Catal. 181 (1999) 280.
[9] IUPAC Reporting physisorption data for gas/solid system, Pure Appl. Chem. 57 (1985) 603.
[10] P. Bonnet, J.M.M. Millet, J. Catal. 161 (1996) 198.
[11] W.P.A. Jansen, M. Ruitenbeek, A.W. Denier, V.D. Gon, J.W. Geus, H.H. Brongersma, J. Catal. 196 (2000) 379.
[12] Y. Inomata, T. Inomata, T. Moriwaki, Spectrochim. Acta 36A (1980) 839.
[13] M. Che, C. Naccache, B. Imelik, M. Prettre, C. R. Acad. Sci., Ser. C 264 (1967) 1901.
[14] H. Knozinger, Adv. Catal. 25 (1976) 184.
[15] C. Mortera, G. Cerrato, Langmuir 6 (1990) 1810.
[16] H.P. Boehm, H. Knøzinger, in: J.R. Anderson, M. Boudart (Eds.), Catalysis Science and Technology, vol. 4, Springer-Verlag, West Berlin, 1983, p. 39.